International Journal of Microwave and Wireless Technologies, 2018, 10(1), 87–91.
doi:10.1017/S175907871700126X

RESEARCH PAPER

A miniaturized evanescent mode HMSIW humidity sensor

CHANG-MING CHEN AND JUN XU

A passive evanescent mode half-mode substrate integrated waveguide (HMSIW) resonator loaded with a complementary split ring resonator (CSRR) is designed and fabricated for humidity sensing applications. The use of the CSRR which is etched on the top plane of the HMSIW can significantly reduce the size of the device. Without any sensing material, the sensor which has a compact size of $0.17\lambda_g \times 0.17\lambda_g$ *can provide high humidity sensitivity up to 5.82 MHz/%relative humidity (RH) at high RH region (>84.3%). The results indicate that the proposed structure is a promising candidate for radio and microwave humidity sensing applications.*

Keywords: Half-mode substrate integrated waveguide (HMSIW), Complementary split ring resonator (CSRR), Humidity sensor

Received 5 May 2017; Revised 30 October 2017; Accepted 31 October 2017; first published online 21 November 2017

I. INTRODUCTION

Recently, many radio frequency identification (RFID) and passive microwave sensors have been successfully explored for humidity detection applications [1–4]. In most cases, humidity sensing material is very crucial since it can determine the sensitivity ability of these types of sensors. However, the use of humidity sensing material will increase the cost and complexity of the sensor fabrication. So, the researchers begin to pay close attention to design passive substrate integrated waveguides (SIWs) humidity sensors, which do not require extra humidity sensing materials [5]. However, this SIWs device usually has the disadvantage of large size, which do not meet the demands of the market to high-performance miniaturized sensors. In 2012, Senior reported half-mode substrate integrated waveguide (HMSIW) resonators, which can easily implement the miniaturization of the devices by utilizing the complementary split ring resonator (CSRR) [6]. More interestingly, Ansari adopted the CSRR-based planar microwave sensors for complex permittivity measurement without any sensing material [7]. So, these useful findings provide an excellent approach for the realization of miniaturized environmental sensors without sensing material. In this paper, a miniaturized planar evanescent mode HMSIW resonator loaded with a CSRR is designed and fabricated for humidity sensing application. The humidity sensing properties of the sensors are discussed and compared with those of the previously reported microwave sensors.

School of Physical Electronics, University of Electronic Science and Technology of China, Chengdu 610054, People's Republic of China. Phone: +86 028 85966249
Corresponding author:
C-M. Chen
Email: ccml_ming@126.com

II. DESIGN PROCEDURE

In order to improve the sensor's sensitivity, a CSRR and the HMSIW cavity are combined in the proposed structure. The CSRR which is etched on the top plane consists of two square slots, a conducting strip between the slots, and a metal patch, as shown in Figs 1(a) and 1(b) shows the lossless equivalent circuit model of the CSRR. C_r represents a capacitance which is induced in the slots by the E-field, and L_r represents an inductance which is induced in the conducting strip and metal patch by the H-field. L_r and C_r can be modeled as a shunt-connected LC resonant tank [8], its resonance frequency is given by

$$f_r = \frac{1}{2\pi\sqrt{L_r C_r}}. \quad (1)$$

C_r can be calculated using the approximate formula of a metallic disk capacitor, while L_r is calculated by using the duality of capacitance and inductance of the SRR model [8]. This LC tank operates at a lower frequency than the cutoff frequency of HMSIW cavity due to evanescent-wave amplification [9]. This characteristic provides a significant size reduction for the sensor. In addition, both the CSRR mode and half-mode of SIW are generated in the cavity because of the effect of the HMSIW combination with a CSRR. Since the quality factor of the CSRR is higher than that of the SIW cavity without the CSRR. Therefore, the humidity sensing performance of the sensor are significantly improved. When water molecules are absorbed by the slots of the CSRR, the variation of the effective capacitance will change the resonance frequency of the CSRR.

The substrate of the resonator is RO5880 with a permittivity of 2.22, loss tangent of 0.0009, and the thickness of 0.508 mm. The dimensions of the resonator are $W =$ 5.3 mm, $W_{50} = 0.76$ mm, $W_1 = 1.75$ mm, $W_2 = 0.54$ mm,

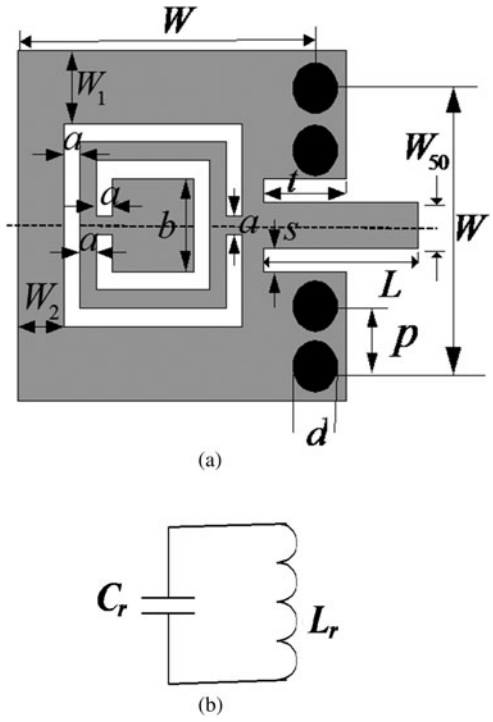

Fig. 1. Structure of the HMSIW resonator sensor: (a) Design parameter of the HMSIW resonator; (b) losses equivalent circuit mode of the CSRR.

$a = 0.25$ mm, $b = 2.35$ mm, $L = 3.9$ mm, $s = 0.1$ mm, $t = 1.4$ mm, $p = 1.5$ mm, and $d = 0.72$ mm. The waveguide cut-off frequency of the HMSIW resonator, f, is approximately given by [10]

$$f = \frac{c}{4W\sqrt{\varepsilon_r}} \tag{2}$$

where W is the effective width of the HMSIW. The resonant frequency of the proposed resonator, f_o, approximately equals f_r, which is mainly determined by the dimensions of the CSRR. f_o is selected to be lower than f due to evanescent wave transmission in the cavity [6].

High-Frequency Structure Simulator (HFSS) was used to simulate the scattering parameters of the proposed structure. Figure 2 shows the simulated S_{11} of the HMSIW cavity with and without a CSRR. From this figure, it can be seen that the

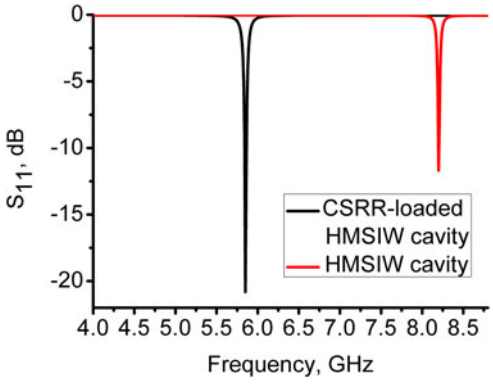

Fig. 2. Simulated S_{11} of the HMSIW cavity (without a CSRR) and CSRR-loaded HMSIW cavity.

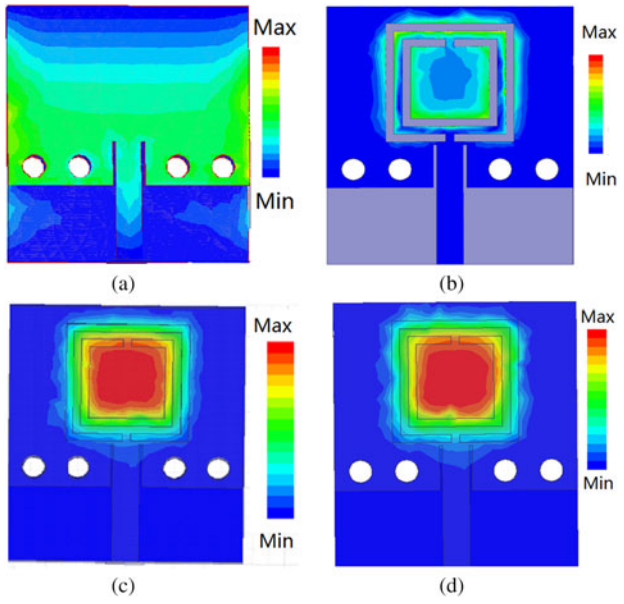

Fig. 3. The E-field distribution: (a) the HMSIW cavity without a CSRR; (b) bottom of the CSRR-loaded HMSIW cavity at 5.82 GHz; (c) top of the CSRR-loaded HMSIW cavity; (d) bottom of the CSRR-loaded HMSIW cavity at 8.2 GHz.

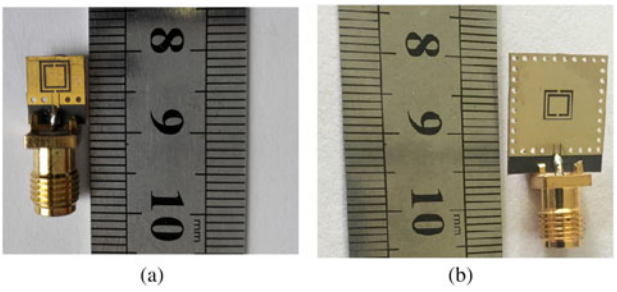

Fig. 4. Images of the fabricated sensors: (a) the HMSIW sensor; (b) the SIW sensor.

f and f_o are about 5.82 and 8.2 GHz, respectively. Figures 3(a) and 3(b) show the E-field distribution of the HMSIW resonator without or with a CSRR structure, respectively. It is found that the higher field concentration is mainly distributed on the fringes of the metalized holes of the resonator for HMSIW cavity, while strong E-field is concentrated on the conductors between the two rings and the inner metal patch of the CSRR-loaded HMSIW sensor. Figures 3(c) and 3(d)

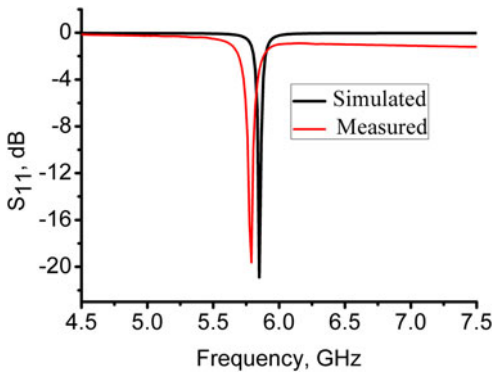

Fig. 5. Simulated and measured S_{11} of the fabricated sensor.

https://doi.org/10.1017/S175907871700126X Published online by Cambridge University Press

Fig. 6. Humidity experimental setup.

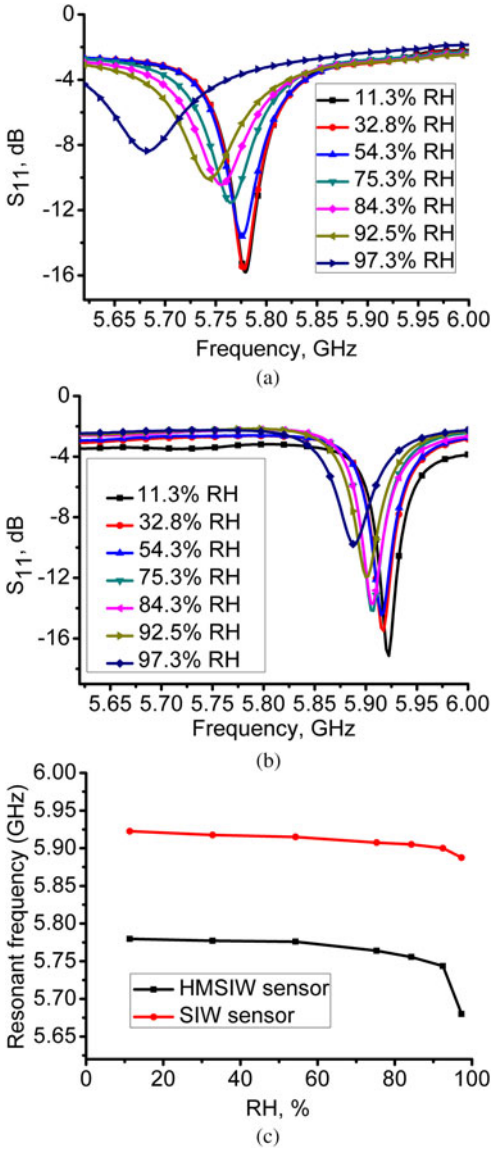

Fig. 7. Measured results of the fabricated sensor at different humidity levels: (a) S_{11} for the HMSIW sensor; (b) S_{11} for the SIW sensor; (c) frequency response of the fabricated HMSIW and SIW sensors.

display the E-field distribution of the CSRR-loaded HMSIW resonator. It can be clearly observed that the magnitude of the E-field inside the cavity is slightly different at 5.82 and 8.2 GHz due to the CSRR perturbation on the HMSIW resonator. The electric coupling of the CSRR decreases the resonance frequency of the cavity without a CSRR. These above-simulated results suggest that the resonance frequency of the resonator will produce a shift by giving an electromagnetic field perturbation on the top or bottom surface of the cavity. A humidity sensor's sensitivity can be estimated by using the dielectric perturbation method [11]. Therefore, the resonator's resonance frequency will produce a shift when the variation of moisture inside the CSRR.

To compare the humidity performance of the CSRR loaded HMSIW sensor and its SIW counterpart, two prototypes are designed and fabricated, as shown in Fig. 4. A vector network analyzer (VNA) (PNA N5244A, Agilent Technologies, USA) is used to measure the S_{11} of the resonator. The microwave experimental system has been calibrated by using an open-short-load mechanical calibration kit (Agilent E8056D) before testing. The output power level of the VNA is set to 0 dBm. Figure 5 shows the simulated and measured S_{11} of the CSRR-loaded HMSIW resonator. The measured resonance frequency is observed at 5.79 GHz. There is a small difference between the simulated and measured results because of the printed circuit board fabrication resolution.

III. HUMIDITY MEASUREMENT

The humidity experimental setup is given in Fig. 6. The port 1 of the VNA is directly connected to the fabricated sensor

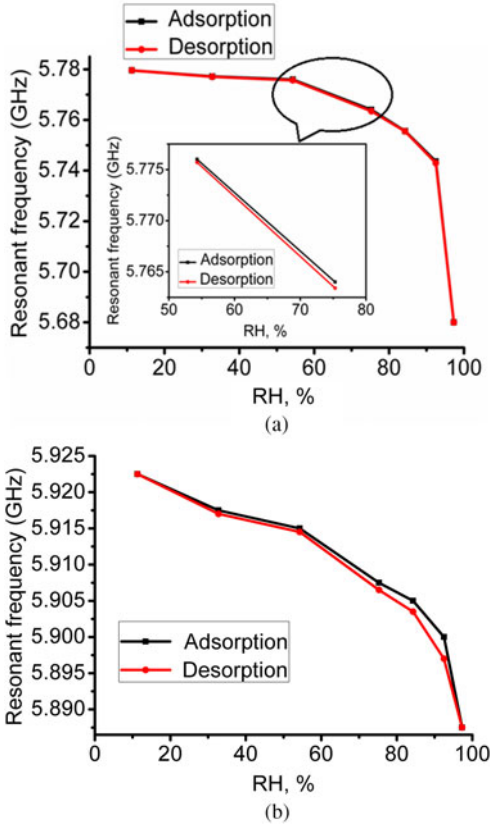

Fig. 8. The humidity hysteresis: (a) HMSIW sensor; (b) SIW sensor.

https://doi.org/10.1017/S175907871700126X Published online by Cambridge University Press

Table 1. Comparison of microwave sensors for humidity sensing.

Refs.	Structure	RH range (%)	Operating frequency (GHz)	Size (λ_g^2)	Sensitive material	Sensitivity (kHz/RH)
[1]	RFID tag	25 ~ 90	0.9	$0.58\lambda_g \times 0.21\lambda_g$	Yes	171
[2]	SIW resonator	11.3 ~ 97.3	3.6	$0.68\lambda_g \times 0.68\lambda_g$	Yes	197
[3]	Coplanar waveguide	30 ~ 90	3.37 or 5.0	Not mentioned	Yes	181
[5]	SIW resonator	0 ~ 80	3.7 or 4.1	$0.7\lambda_g \times 0.7\lambda_g$	No	101
This work	Evanescent mode HMSIW resonator	11.3 ~ 97.3	5.82	$0.17\lambda_g \times 0.17\lambda_g$	No	312@ (11.3% ~ 84.3%) 5820@ (84.3% ~ 97.3%)

through a soft coaxial cable. Saturated LiCl, $MgCl_2$, $Mg(NO_3)_2$, NaCl, KCl, KNO_3, and K_2SO_4 solutions at 25°C were approximately yield ~11.3, 32.8, 54.3,75.3, 84.3, 92.5, and 97.3% relative humidity (RH) levels, respectively. Due to the presence of moisture inside the slots of the CSRR, the effective permittivity of the dielectric will be changed, resulting in a frequency shift for the resonator. It is noted that the experiment is repeated for 4 days and the readings are obtained under the same experimental conditions.

IV. RESULTS AND DISCUSSION

The measured S_{11} of two sensors as a function of frequency at different humidity levels are plotted in Figs 7(a) and 7(b). It can be clearly found that the measured resonance frequency of each sensor decreased with the RH level increased. Also, the peak magnitude of $|S_{11}|$ of the sensor decreased with increasing RH. The measured humidity sensitivity S of the HMSIW resonator is given by [12]

$$S = \left|\frac{\Delta f_r}{\Delta \%RH}\right| \tag{3}$$

where $\triangle f_r$ is frequency shift and △%RH is the corresponding change of RH. Figure 7(c) plots the frequency response of the two sensors with the RH levels. Examination of the figure shows that the frequency shift of the HMSIW sensor is obviously larger than that of the SIW sensor in the range 11.3–97.3%RH. According to equation (3), the measured humidity sensitivity of the HMSIW sensor and SIW sensor are 312 kHz/%RH and 239 kHz/%RH in the RH range of 11.3–84.3%, respectively. When humidity changed from 84.3 to 97.3%, the HMSIW sensor can provide high humidity sensitivity up to 5.82 MHz/%RH that is about five times compared with the SIW humidity sensor. This result indicates that our sensor is more suitable for the high RH detection since it has large sensitivity at high RH region. The enhanced sensitivity of the HMSIW sensor can be interpreted as follows: (1) the introduction of the CSRR structure can effectively increase the numbers of adsorbed water molecules on the surface of the substrate, resulting in the increase of the effective dielectric constant [5]. Thus, the equivalent capacitance of the shunt LC resonant tank will increase with increasing RH levels; (2) the fringe E-field of the HMSIW sensor can also increase the equivalent capacitance of the LC resonant tank. These two factors will significantly decrease the resonant frequency of the CSRR-loaded HMSIW humidity sensor, i.e. the increase of the humidity sensitivity.

Humidity hysteresis characteristics of the proposed sensors were also measured. The sensors were first placed in the RH-increasing environment for water absorption, and then exposed to the RH-decreasing environment for water desorption. Figure 8 plots the humidity hysteresis curves of two sensors. It can be found that the humidity hysteresis effect is not patent in the range of 11.3%RH–97.3%RH for the HMSIW sensor. The inset of the Fig. 8(a) shows the small difference between the curves of the adsorption and desorption. From the Fig. 8(b), it can be seen that the maximum humidity hysteresis of the SIW sensor occurred at nearly 92.5%RH and was about ~3%RH. Obviously, the HMSIW sensor has the lowest humidity hysteresis than the SIW sensor. This result indicates that water molecules adsorption and desorption do not introduce excessive dielectric losses for the HMSIW sensor.

Previous microwave humidity sensors with or without sensing material were reported in the literature. Table 1 lists the humidity performance comparison between the proposed evanescent mode HMSIW sensor and other microwave humidity sensors. It can be observed that most of the RF or microwave humidity detection structures with sensing material achieved sensitivity in the order of several hundreds of kHz/RH. While our proposed sensor without any sensing material can provide the advantages of high sensitivity, wide humidity detection range, and compact size. This indicates that the proposed compact sensor is more convenient for passive sensing applications.

V. CONCLUSION

In this paper, we proposed a miniaturized evanescent mode HMSIW humidity sensor loaded with a CSRR. Without any sensing material, the sensor which has a compact size of $0.17\lambda_g \times 0.17\lambda_g$ can provide high humidity sensitivity up to 5.82 MHz/%RH at high RH region (>84.3%). The proposed structure can be a good candidate to implement high sensitivity microwave passive sensors for humidity sensing applications.

ACKNOWLEDGEMENTS

This work was supported by the National Natural Science Foundation of China (grant no. 61401047).

REFERENCES

[1] Virtanen, J.; Ukkonen, L.; Björninen, T.; Elsherbeni, A.Z.; Sydänheimo, L.: Inkjet-printed humidity sensor for passive UHF RFID systems. IEEE Trans. Instrum. Meas., **60** (8) (2011), 2768–2777.

https://doi.org/10.1017/S175907871700126X Published online by Cambridge University Press

[2] Chen, C.; Xu, J.; Yao, Y.: SIW resonator humidity sensor based on layered black phosphorus. Electron. Lett., **53** (4) (2017), 249–251.

[3] Kim, Y.; Jang, K.; Yoon, Y.; Kim, Y.J.: A novel relative humidity sensor based on microwave resonators and a customized polymeric film. Sens. Actuators B, **117** (2006), 315–322.

[4] Amin, E.M.; Bhuiyan, M.S.; Karmakar, N.C.; Jensen, B.W.: Development of a low cost printable chipless RFID humidity sensor. IEEE Sens. J., **14** (1) (2014), 140–149.

[5] Matbouly, H.E.; Boubekeur, N.; Domingue, F.: Passive microwave substrate integrated cavity resonator for humidity sensing. IEEE Trans. Microw. Theory Techn., **63** (12) (2015), 4150–4156.

[6] Senior, D.E.; Cheng, X.; Yoon, Y.K.: Electrically tunable evanescent mode Half-mode substrate-integrated-waveguide resonators. IEEE Microw. Wirel. Compon. Lett., **22** (3) (2012), 123–125.

[7] Ansari, M.A.H.; Jha, A.K.; Akhtar, M.J.: Design and application of the CSRR-based planar sensor for noninvasive measurement of complex permittivity. IEEE Sens. J., **15** (12) (2015), 7181–7189.

[8] Baena, J.D. et al.: Equivalent circuit models for split ring resonators and complementary split ring resonators coupled to planar transmission lines. IEEE Trans. Microw. Theor. Tech., **53** (10) (2005), 1451–1461.

[9] Dong, Y.D.; Yang, T.; Itoh, T.: Substrate integrated waveguide loaded by comple-mentary split-ring resonators and its applications to miniaturized waveguidefilters. IEEE Trans. Microw. Theor. Tech., **57** (9) (2009), 2211–2223.

[10] Senior, D.E.; Cheng, X.; Machado, M.; Yoon, Y.K.: Single and dual band bandpass filters using complementary split ring resonator loaded half mode substrate integrated waveguide, in Proc. IEEE Antennas Propag. Symp., Toronto, ON, Canada, July 2010, 1–4.

[11] Xu, F.; Wu, K.: Guided-wave and leakage characteristics of substrate integratedwaveguide. IEEE Trans. Microw. Theor. Tech., **53** (2005), 66–73.

[12] Chang, K.; Kim, Y.H.; Kim, Y.J.; Yoon, Y.J.: Functional antenna integrated with relative humidity sensor using synthesized polyimide for passive RFID sensing. Electron. Lett., **43** (3) (2007), 7–8.

Chang-Ming Chen was born in Sichuan, China. He received his MS degree from the School of Physical Electronics, University of Electronic Science and Technology of China, China in 2006. He is currently pursuing his Ph.D. degree at the School of Physical Electronics, University of Electronic Science and Technology of China (UESTC). His current research interests include microwave and millimeter-wave sensors.

Jun Xu was born in Sichuan, China. He is currently a Professor in the School of Physical Electronics, University of Electronic Science and Technology of China (UESTC). His current research interests include microwave and millimeter-wave circuits and system.

https://doi.org/10.1017/S175907871700126X Published online by Cambridge University Press